J. Adv. Model. Earth Syst., **Vol. 2**, Art. #6, 20 pp. Review Article

Progress in Understanding Land-Surface-Atmosphere Coupling from LBA Research

Alan K. Betts[1] *and Maria Assunção F. Silva Dias*[2]

[1] Atmospheric Research, Pittsford, VT, USA
[2] Department of Atmospheric Science, University of São Paulo, SP, Brazil

Manuscript submitted 12 November 2009; in final form 6 June 2010

LBA research has deepened our understanding of the role of soil water storage, clouds and aerosols in land-atmosphere coupling. We show how the reformulation of cloud forcing in terms of an effective cloud albedo per unit area of surface gives a useful measure of the role of clouds in the surface energy budget over the Amazon. We show that the diurnal temperature range has a quasi-linear relation to the daily mean longwave cooling; and to effective cloud albedo because of the tight coupling between the near-surface climate, the boundary layer and the cloud field. The coupling of surface and atmospheric processes is critical to the seasonal cycle: deep forest rooting systems make water available throughout the year, whereas in the dry season the shortwave cloud forcing is reduced by regional scale subsidence, so that more light is available for photosynthesis. At sites with an annual precipitation above 1900 mm and a dry season length less than 4 months, evaporation rates increased in the dry season, coincident with increased radiation. In contrast, ecosystems with precipitation less than 1700 mm and a longer dry season showed clear evidence of reduced evaporation in the dry season coming from water stress. In all these sites, the seasonal variation of the effective cloud albedo is a major factor in determining the surface available energy. Dry season fires add substantial aerosol to the atmosphere. Aerosol scattering and absorption both reduce the total downward surface radiative flux, but increase the diffuse/direct flux ratio, which increases photosynthetic efficiency. Convective plumes produced by fires enhance the vertical transport of aerosols over the Amazon, and effectively inject smoke aerosol and gases directly into the middle troposphere with substantial impacts on mid-tropospheric dispersion. In the rainy season in Rondônia, convection in low-level westerly flows with low aerosol content resembles oceanic convection with precipitation from warm rain processes and little electrification. But in the same region in the dry season, widespread fires produce a high aerosol loading with high numbers of cloud condensation nuclei from biomass burning; and convection is then dominated by ice-phase processes giving deep clouds with frequent lightning and convective tops in the lower stratosphere. Recent studies based on measurements of CCN and cloud droplet distributions have successfully modeled this wide range of convective regimes, and shown the fundamental link between cloud droplet spectra, convective structure and precipitation. The regional scale circulation responds to precipitation and aerosol forcing, as well as the memory provided by soil moisture. The field observations from LBA have been essential to identifying the interactions of critical processes, and for the development and evaluation of our models of the coupled system.

DOI:10.3894/JAMES.2010.2.6

1. Introduction

More than a decade has passed since Betts et al. (1996) published a paper reviewing the land-surface-atmosphere interaction from modeling and observational perspectives. Since then many field campaigns have increased our understanding, and models have grown in complexity to represent more of the interactive physical processes. Betts (2009) addresses some general issues using some field data, but primarily using data from the European Centre for Medium Range Weather Forecasts (ECMWF) model. The purpose of this paper (which is largely but not entirely a review) is to specifically document the progress in our

To whom correspondence should be addressed.
Alan K. Betts, Atmospheric Research, Pittsford, VT, USA
akbetts@aol.com

understanding that has come from LBA, the Large Scale Biosphere-Atmosphere Experiment in Amazônia (LBA, 1996; Keller et al. 2004). Amazônia is an important equatorial climatic region, where cloud cover and precipitation, but not temperature, have a large seasonal variation. Rainforest is the natural ecosystem (for most of the region), but areas have been deforested to become pasture or agricultural land. This land-use change has altered not only the surface albedo and roughness, but seasonal biomass burning has a large impact on the atmospheric composition; which in turn affects both radiative absorption and scattering, net ecosystem exchange and through microphysical processes, convective structure and rainfall. The future of Amazônia with its large forest carbon stocks and biodiversity is a key issue as global climate changes.

Planning for the LBA experiment started in the middle 1990's and the field phase began in 1998 as an international effort between Brazil, Europe and the United States to understand the functioning of the several Amazon ecosystems and the role of Amazônia in global climate. From the beginning many components were planned: long-term monitoring of the surface energy and carbon fluxes using flux towers (currently there are 12); and a series of intensive field campaigns to understand the biosphere-atmosphere interactions, with a focus on cloud and boundary layer processes, including one in Rondônia in the wet season in 1999 and one in 2002 during the dry-to-wet transition season. Since the beginning, the scientific management of LBA has been in the hands of an international science steering committee with a rotating chair. The LBA project office in Manaus is responsible for the project management. Research and building scientific infrastructure in Amazônia go hand-in-hand, and more than 250 students have been awarded doctoral degrees funded by LBA over the past ten years. Initially, major funding in Brazil came from the Ministry of Science and Technology (MCT) and from the state of São Paulo Research Foundation (FAPESP); as well as from grants from the European Union and NASA. The project was originally driven by the scientific community; but in time MCT recognized its importance to the Brazilian Amazon and from 2007 has ensured that the long term monitoring infrastructure receives regular federal funding. Based on the results of the first phase, LBA is now starting a second phase, where most of the emphasis is on the changing environment as a result of human induced pressures and global climate variability and change. More information on the project may be found at http://lba.inpa.gov.br.

Many aspects of our understanding of the coupling of processes between the land-surface and the atmosphere have benefited from LBA; including rooting and sub-surface soil processes, boundary layer development, radiative, convective, biogeochemical and microphysical interactions with aerosols and clouds; and the coupling between mesoscale convective structure and the large-scale flow. We will not cover all aspects here - some are addressed in more depth in the chapters of a recent LBA book, *Amazonia and Global Change* (Keller et al. 2009). In this book, Nobre et al. (2009) summarize our understanding of the main features of the Amazonian climate. Da Rocha et al. (2009b) review measurements of sensible and latent heat at seven flux towers across Amazônia. Betts et al. (2009b) discuss the interaction between the surface climate, the boundary layer and larger-scale circulations. Longo et al. (2009) address some impacts of biomass burning on regional transports of smoke. Marengo et al. (2009) review the long-term climate variability of the Amazon and the projected climate-vegetation feedback from global warming and climate change. Silva Dias et al. (2009) discuss the regional and remote impact of deforestation on climate.

Our starting frame of reference for discussing progress in understanding is a diagram of the coupling of physical processes in Betts et al. (1996), which is reproduced here as Figure 1 in section 2. We will discuss extensions of this diagram to include additional feedback loops that have emerged more clearly from LBA research, and given us a more detailed picture of the land-surface-atmosphere interactions over the Amazon. In section 3 we will look at the role of cloud forcing in the surface energy budget; and map the relation between near-surface relative humidity, effective cloud albedo, longwave net radiation and the diurnal temperature range. In section 4 we look at land-surface processes, their seasonal cycle and their climate impacts; discuss progress in modeling surface and sub-surface processes, and our understanding of the forest to savannah gradient, including the role of clouds in determining the gradient of net radiation across the biome. Section 5 reviews some important aerosol issues: the modeling of plume fires, the modeling of aerosol-cloud-precipitation coupling and the radiative impacts of aerosol on the circulation. Much progress has been made in understanding the details of physical processes and their interactions over the Amazon. Nonetheless, accurate representation of the coupling between clouds and the surface energy balance, the diurnal cycle of convection, and the coupling between aerosols, convective precipitation, the large-scale circulation and the climate still present modeling challenges.

2. Coupling of Physical Processes

Figure 1, adapted from Betts et al. (1996), summarizes some of the links between the surface energy budget, the surface energy partition into sensible (H) and latent heat (LE) fluxes, which drive the boundary layer (BL) evolution and generate clouds; which in turn modify the surface radiation budget, sometimes giving precipitation which modifies soil moisture. Three important timescales were suggested: the fast diurnal response of the surface, BL and clouds, the slower response of the sub-surface, which responds to precipitation events, but has important trends over the season; and a single arrow was included for the production of aerosols from biomass burning on century timescales.

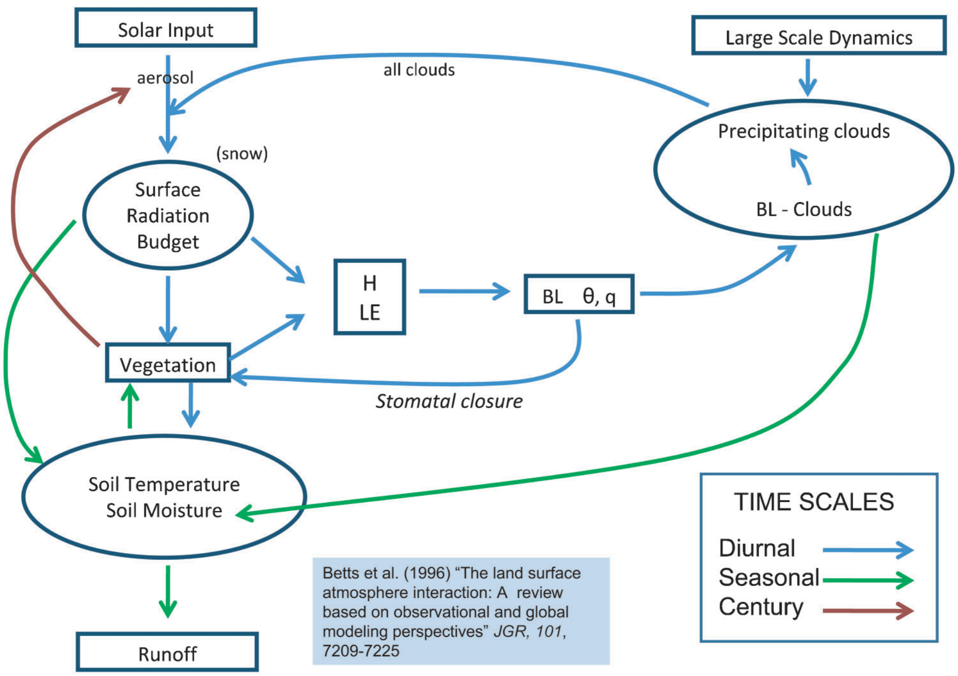

Figure 1. Schematic of land-surface-atmosphere coupling from Betts et al. (1996)

This was drawn with the timescale for the natural burning and regrowth of the boreal forests in mind.

Figure 2 retains the structure of Figure 1, but it has many additions and modifications, which have emerged from a decade of LBA research. The surface and atmosphere over Amazônia form a highly coupled system. At the surface, evaporation, carbon exchange and biomass burning are important; while in the atmosphere, aerosols, condensation nuclei, clouds and precipitation interact. Atmospheric composition, clouds and aerosols determine the direct and diffuse radiation field, which links surface, atmosphere and the top-of-the-atmosphere radiation budgets. Specifically Figure 2 reflects our deeper understanding of the role of

1) Clouds and aerosols in the shortwave (SW) and longwave (LW) radiation budget and their links to the surface, BL climate and diurnal temperature range (DTR).
2) Impact of diffuse radiation from aerosols and clouds and deep rooting on net ecosystem exchange (NEE).
3) Convection in the transport of other atmospheric species including CO_2 and aerosols.
4) Surface emissions and aerosols in the microphysics of clouds and precipitation.
5) The coupling between clouds, mesoscale dynamics and atmospheric structure.
6) Land-use and land cover

We will cover aspects of topics 1) to 4) (except for CO_2 transports); and as a guide, these are high-lighted in red on Figure 2. We address the impact of clouds on the surface SW and longwave LW radiation budget, and the coupling between lifting condensation level (LCL), net LW radiation and DTR (section 3). We discuss the importance of deep rooting on the seasonal cycle and the enhancement of NEE by diffuse radiation scattered by aerosols (section 4). A few specific aerosol topics: biomass burning, surface emissions and the atmospheric transport of aerosols, and the impact of high aerosol loading on convective dynamics and precipitation through cloud microphysical changes are covered in section 5.

In this short review we will not discuss the coupling between clouds, mesoscale dynamics and atmospheric structure (topic 5). We will address the current biome gradient from forest to savannah, but otherwise we shall not discuss land cover issues (topic 6). Deforestation in the Amazon plays a significant role in the local climate and affects all these processes. Silva Dias et al. (2009) and Betts et al. (2009b) contain some discussion of the impact of deforestation on local and regional circulations. Note that we have reduced the longest timescale to decadal to reflect the faster human-driven land-use change of the Amazonian landscape and on greenhouse gas emissions.

Our reductionist approach to modeling the earth system faces a fundamental difficulty. We have to identify important processes from observational analyses, before they can be introduced into models in the form of detailed sub-models and parameterizations. However this increases complexity, and the overall behavior of the fully coupled system depends on the parameters of all these sub-models. So observations of the behavior of the coupled system on different time and space-scales are essential to constrain models.

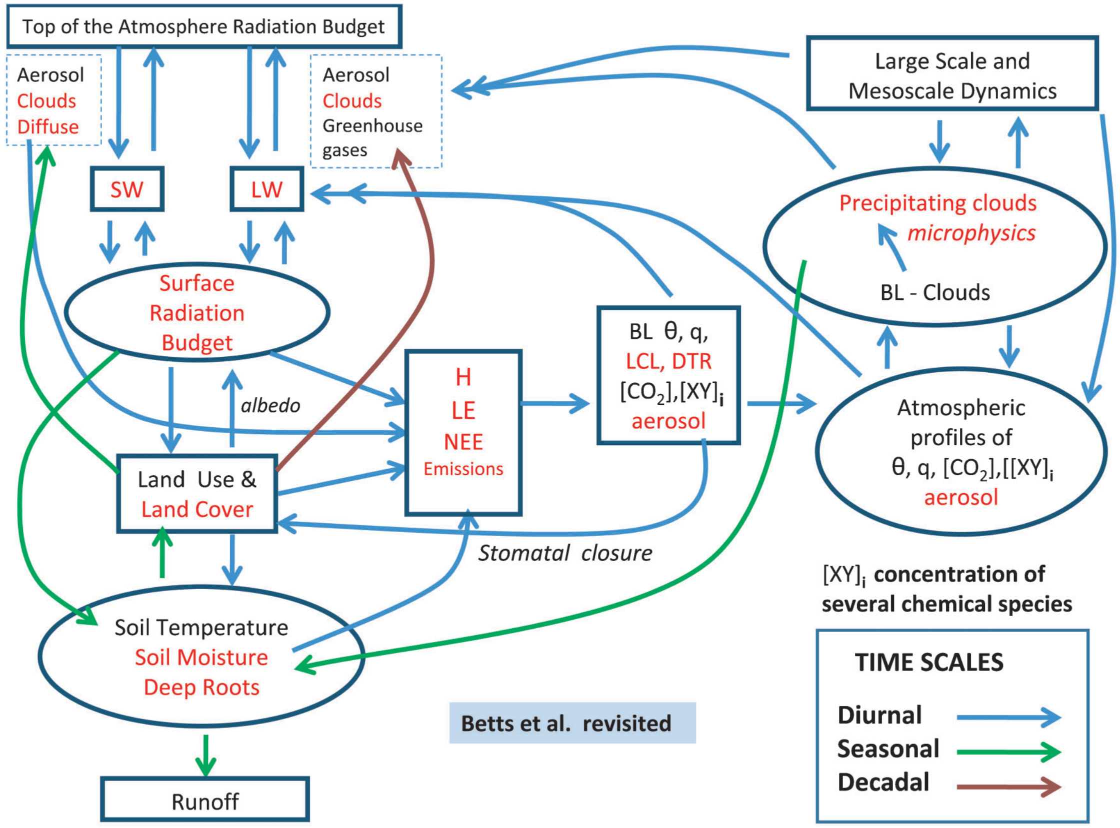

Figure 2. Update of Figure 1, based on LBA research.

3. Coupling of clouds to surface and boundary layer processes

Figure 1 from Betts et al. (1996) recognized that clouds impacted the hydrologic cycle through the surface radiation budget, but at that time the quantitative impact on the separate LW and SW budgets in the tropics was poorly understood. In addition, the importance of the tight coupling between surface transpiration, boundary layer (BL) cloud and net radiation was little appreciated (see Betts, R. et al. 2004). Across the Amazon, seasonal cloud variability is critical to the surface radiation budget and photosynthetic uptake. So in this section, we start by looking at the coupling between clouds, the surface energy budget and the surface climate, represented by daily averaged quantities and the diurnal temperature range. Our conceptual framework uses the effective cloud albedo, which emerged from studying land-surface coupling for the Madeira river basin (Betts and Viterbo, 2005). Data from the Rebio Jaru forest site and the Fazenda Nossa Senhora (FNS) site in Rondônia, collected during LBA between 1999 and 2002 (von Randow et al. 2004) will be used for illustration. The figures in this section have not been previously published (although they were presented at the Manaus LBA meeting in 2008).

3.1 Surface energy budget

The surface energy balance (SEB) has a large impact on the surface equilibrium climate and the diurnal temperature range. It is traditionally simplified as

$$Rn = SW_{net} + LW_{net} = H + LE + G \qquad (1)$$

where the surface net radiation, Rn, is the sum of net shortwave and longwave fluxes; and it is balanced by the upward sensible heat flux, H, and latent heat flux, LE, and the storage, G, in the ground and the vegetation canopy. We neglect the small amount of energy taken up by photosynthesis. Eq. (1) for the SEB is a highly coupled system, but we shall break it into some components to clarify the role of different processes. We first introduce an 'effective cloud albedo', to quantify the poorly understood role of clouds in the surface SW budget. Then we shall look at the dependence of the DTR on LW_{net}, and the interdependence of LW_{net} on humidity and effective cloud albedo.

3.2 Conversion of SW cloud forcing to effective cloud albedo

How to quantify the role of the cloud field in the SEB is a fundamental issue in land-atmosphere coupling. This is especially important for tropical systems where surface, BL and clouds are tightly coupled. Although clouds are ubiquitous, often they are poorly measured and modeled. Studies of the land-surface coupling for the Madeira river basin (Betts and Viterbo, 2005) using ECMWF reanalysis (ERA-40) data (Uppala et al. 2005) led to the reformulation of the surface shortwave radiation budget in terms of an *effective cloud albedo* defined by normalizing the surface short-wave cloud forcing, SWCF, by the downwelling clear-sky flux, SW_{down}(clear)

$$\alpha_{cloud} = -\,SWCF/SW_{down}(clear) \tag{2}$$

where

$$SWCF = SW_{down} - SW_{down}(clear) \tag{3}$$

This then gives a symmetric representation of the surface SW_{net} in terms of two albedos

$$\begin{aligned} SW_{net} &= SW_{down} - SW_{up} \\ &= (1-\alpha_{surf})(1-\alpha_{cloud})SW_{down}(clear) \end{aligned} \tag{4}$$

where the familiar surface albedo, α_{surf}, is the ratio SW_{up} / SW_{down}. The effective cloud albedo, α_{cloud}, can be used to compare models and data and evaluate land-surface coupling. Aerosols also have a significant impact on the clear-sky flux, particularly in the dry season, when forest and agricultural burning is greatest. In the past, numerical models often used a climatic aerosol specification, but recently as aerosol analyses are being introduced (see section 5), models have started to output both *clean-sky* (without aerosols) and *clear-sky* radiative fluxes (with aerosols).

This effective cloud albedo α_{cloud} is just a non-dimensional measure of the surface shortwave cloud forcing, which depends on cloud fraction as well as cloud reflectivity and absorption. Note that we call this an *effective* cloud albedo, because coming from the SWCF, it is per unit area of the surface, not per unit area of cloud. Errors in α_{cloud} in models may come either from errors in cloud fraction or in the representation of cloud microphysics that determine cloud albedo. However, the observed variability of α_{cloud} is dominated typically by the variability of cloud fraction, rather than cloud albedo.

In the surface SW budget, the two albedos play equivalent roles: α_{surf} is a function of surface properties, and may vary seasonally with vegetation cover (and with snow at high latitudes); while α_{cloud} is a function of boundary layer and tropospheric clouds, with variability on a wide range of timescales. However in the tropics, most of the cloud field is at least partially coupled to the sub-cloud layer moisture on diurnal time-scales.

3.3 Effective cloud albedo from Rondônia data

Figure 3 illustrates the transformation to effective cloud albedo. The upper panels show the ERA-40 daily clear sky flux and the measured daily mean SW_{down} flux at two sites in Rondônia: the Jaru forest site and the FNS pasture site. The dry season lasts three months (June, July and August). The location of the Jaru site is shown on Figure 6 (in section 4.5, later), where we discuss some aspects of the biome gradient across the Amazon. The pasture site is about 88 km to the southwest of the Jaru forest site. The gap by which the measured fluxes lie below the ERA40 clear-sky estimate is a measure of the cloud forcing given by (3); although some of this gap in August and September is likely due to the underestimation of aerosols in the ERA-40 clear sky calculation. ERA-40 uses a fixed monthly climatology for aerosols. In section 5, we will show an example of more recent experimental aerosol analyses in the dry season. We made small corrections ($<1\%$) to the ERA-40 clear sky flux to account for the small latitude differences between the ERA-40 grid-box center (10.65°S) and the two sites at (10.08, 10.75°S).

The lower panels are the transformation given by (2) from cloud forcing to effective cloud albedo. We see that at the peak of the dry season in July, there is 6% more reflective cloud over the pasture site, as found by previous authors (Cutrim et al. 1995; Wang et al. 2009). The pasture site has an 8% higher surface albedo, as well as more reflective cloud, which leads to a reduction in Rn by about 14% in the dry season (von Randow et al. 2004).

Different calculations of SW_{down}(clear) vary considerably. Betts et al. (2009a) compared SW_{down}(clear) over the Amazon from ERA-40, from a more recent 'interim reanalysis', ERA-Interim (Uppala et al. 2008), and the independent estimate (Zhang et al. 2004) from the International Satellite Cloud Climatology Project (ISCCP). In the dry season SW_{down}(clear) is about 20 W m^{-2} greater in ERA-40 than in ERA-Interim, which has updated radiation codes and a different aerosol climatology, but a substantially larger surface cold humid bias with respect to observations than ERA-40 (Betts et al. 2009a). The ISCCP SW_{down}(clear) is closer to ERA-Interim in the dry season and to ERA-40 in the wet season. For the observations, there is uncertainty in the absolute calibration of the radiometers: for example, an uncertainty of 10 W m^{-2} in the SWCF in the dry season corresponds to a 4% uncertainty in α_{cloud}.

We use SW_{down}(clear) from ERA-40 in Figure 3, because the corresponding lower clear-sky values from ERA-Interim are well below the observations on many clear days, so these ERA-Interim estimates and the observations are simply incompatible. We shall also use ERA-40 for clear-sky net radiation in section 4.5, because the ERA-Interim values are lower than the observations in near clear-sky conditions.

3.4 Links between RH, cloud, LW_{net} and diurnal temperature range

Studies using reanalysis model data have also shown that there is a link between diurnal temperature range (DTR) and the daily mean LW_{net} cooling of the surface (Betts 2004, 2006). Figures 4(a) and (b) illustrate this for the

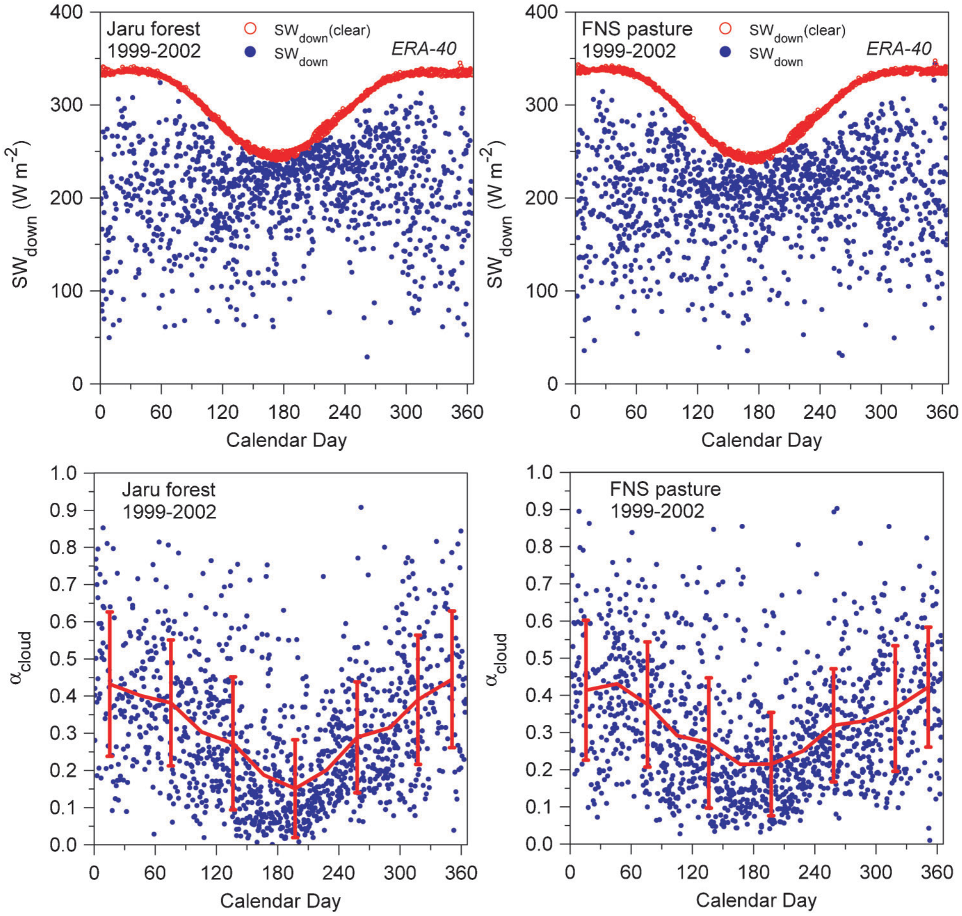

Figure 3. Daily mean incoming SW_{down} flux at Jaru forest site and FNS pasture in Rondonia (upper panels), with clear-sky flux from ERA-40 and (lower panels) transformation to daily effective cloud albedo with monthly means shown. The error bars, shown every other month, are the standard deviation of the daily values.

Rondônia sites, with a partition between dry season (JAS, July, August, September) and wet season (DJFMAM, December to May). For both seasons there is a quasi-linear decrease in the DTR with decreasing outgoing LW_{net}, although the DTR is higher in the dry season when daily precipitation is less.

Figure 4 (c) and (d) show the relation between surface relative humidity (RH), effective cloud albedo and LW_{net}. The clear-sky LW_{net} again comes from ERA-40. The LW cooling of the surface is reduced with higher RH (and lower cloud-base) and with higher cloud cover, represented here by the effective cloud albedo. The small vertical shift of the data between panels (c) and (d) is likely to be due to calibration differences between the LW radiometers. The linear regression of LW_{net} on RH and effective cloud albedo explains 69% (77%) of the variance for the forest (pasture) site (not shown).

Using the ERA-40 data alone, we can approximately fit the longwave cloud forcing (LWCF) to effective cloud albedo in the form

$$\begin{aligned} LWCF &= LW_{net} - LW_{net}(clear) \\ &\approx -\alpha_{cloud}\, LW_{net}(clear)/1.3 \end{aligned} \qquad (5)$$

This fit explains about 67% of the variance of LWCF.

3.5 Stratification by cloud albedo

Betts et al. (2006) showed that the effective cloud albedo could be used to explore relations between cloud forcing and surface processes in boreal forest data. This framework is also useful in Amazônia. Figure 5 shows the relationship of some near-surface variables to effective cloud albedo for these sites in Rondônia. Figures 5a) and c) show P_{LCL}, the pressure height of the Lifting Condensation Level (LCL) and with slight approximation relative humidity, RH, as a function of effective cloud albedo. These observations show clearly that there is a coupling between cloud-base and cloud cover, and this relationship is much tighter in the wet season than in the dry season.

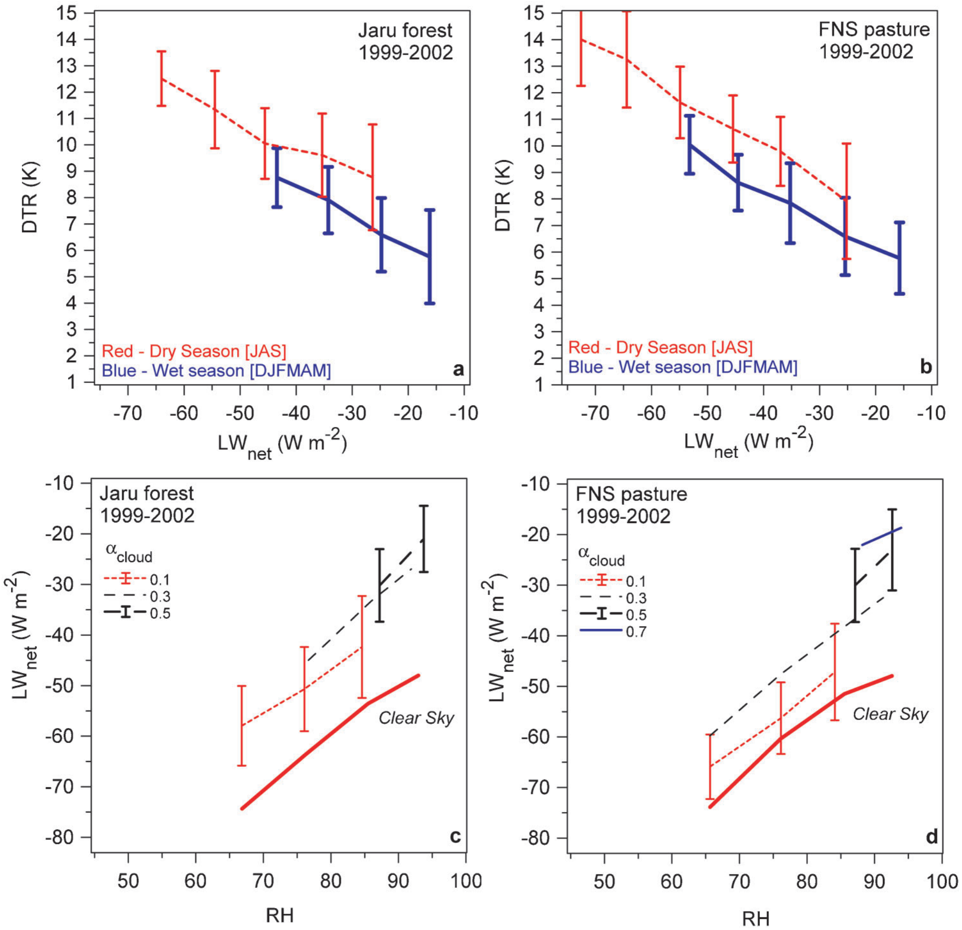

Figure 4. (a) (b) Relation between LW_{net} and diurnal temperature range for dry and wet seasons; (c) (d) Dependence of LW_{net} on RH and α_{cloud}. The error bars are the standard deviation of the binned data.

Figures 5c) and d) show the stratification of maximum, mean and minimum temperature and DTR with effective cloud albedo. There is a quasi-linear decrease of DTR with α_{cloud}, consistent with Figures 4a) and b), given the relation between LW_{net}, RH and α_{cloud}. The upper curves show that, except at low α_{cloud}, DTR decreases because T_{max} decreases; while T_{min} changes little with increasing α_{cloud} for these sites in Rondônia.

We started section 3 by scaling the SWCF to give an effective cloud albedo. Then we showed that the DTR is tightly coupled to LW_{net}, which is turn is coupled to RH and effective cloud albedo. In fact the longwave cloud forcing can be approximated in terms of effective cloud albedo and the clear-sky net longwave flux. Given all these interconnections, the DTR has a nearly linear relation to effective cloud albedo. In fact convection and much of the cloud field over the Amazon are almost always coupled to the sub-cloud layer in the daytime. Consequently, on daily timescales, the SWCF and LWCF, the surface energy budget, the near-surface climate, the diurnal temperature range and cloud-base together form a tightly coupled system, which responds to the large-scale atmospheric forcing of mean ascent or descent over the region. At the time Figure 1 was drafted, the details of all these links were poorly appreciated. The extra details shown in red in Figure 2 are an indication of our much deeper current understanding of the tightly coupled land-surface-BL-cloud system.

4. Land-surface processes and climate impacts

Vegetation is highly dependent on solar radiation, temperature and soil moisture (Mahli et al. 1999) with near-step functions describing the thresholds of plant functioning under stress or unavailability of vital resources. Local climate is linked to vegetation type and dynamics through their effects on surface temperature, atmospheric moisture, cloudiness and ultimately on rainfall. Furthermore, the complex interaction between vegetation and local climate is also a function of soil type, latitude, distance from the sea shore, and large-scale atmospheric weather systems, especially the tropical circulation. One of the main concerns for the adequate modeling of vegetation dynamics is not only its effects on local weather and climate, but also the impact on the Earth's carbon balance, which is in turn linked to global

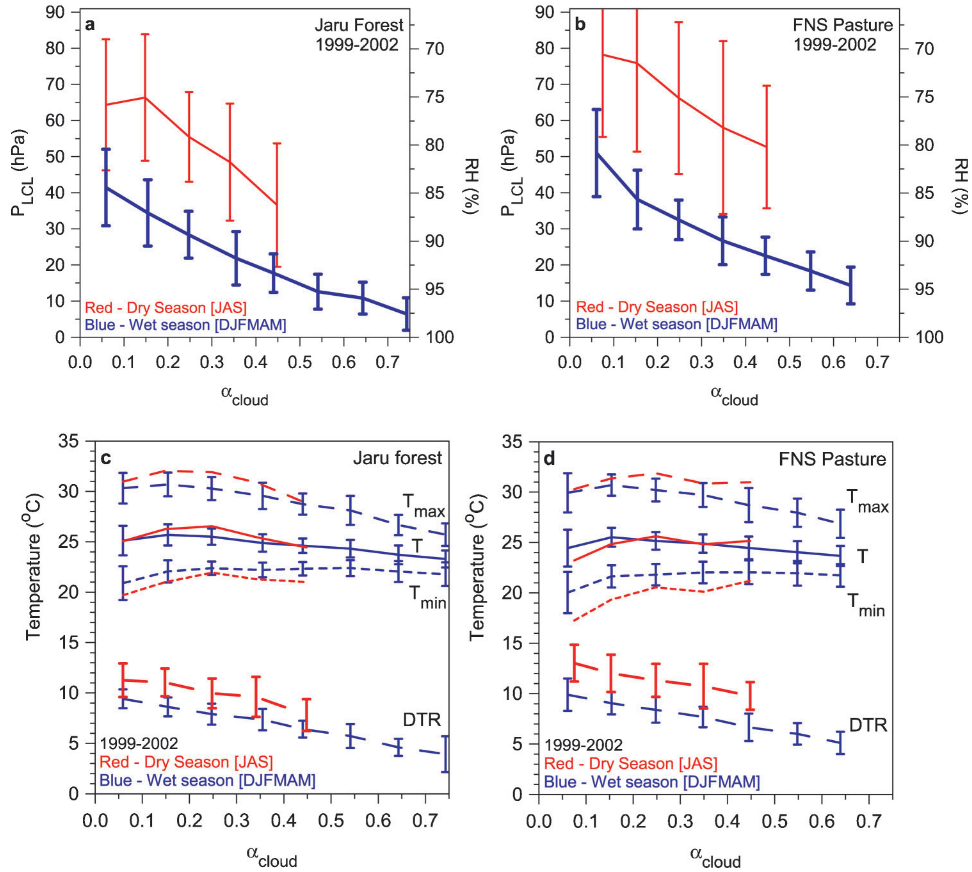

Figure 5. (a) (b) Relation of daily mean LCL and RH; (c) (d) daily maximum, mean and minimum temperatures and DTR to daily mean cloud albedo.

warming and a probable severe perturbation of the global climate (IPCC, 2007). The Amazon Basin tropical forest and its boundaries with agricultural lands and tropical savannah (*cerrado*) present a major challenge to modeling vegetation-climate feedback dynamics in future climate scenarios. In a warmer and moister climate, with higher atmospheric carbon dioxide concentration, the forest could undergo an enhanced growth that would represent a sink for the atmospheric carbon, with enhanced carbon storage in soils and trees, in approximately equal amounts. However a warmer climate would also induce stronger respiration from the soils that would be a source of carbon for the atmosphere. In addition, changes in cloudiness and rainfall, which are likely to occur accompanying the changing regional climate, result in a very delicate balance that can tip either way as tropical forests and neighboring landscapes seek a new state of equilibrium (Betts, R. et al. 2004; Cox et al. 2004; Marengo et al. 2009). Land-use changes are yet another factor.

We will not address here the future climate issue, nor changes in land-use. However, in the last 10 years of LBA research, several new aspects of the vegetation dynamics in the Amazon Basin have been observed in detail, that have been added to Figure 2. We will review what has been learnt, because these discoveries have had a profound impact on our representation of the climate-vegetation interaction in models that is still ongoing. In section 4.5 we will again comment on the importance of the coupling of the surface radiation balance to the cloud field.

4.1 Seasonality of ET and NEE in old-growth forest.

Earlier studies had shown that there was little seasonal variation in evapotranspiration (ET) at Manaus (Roberts et al. 1993), which has only a brief 2-month dry season. The length of dry season is usually defined as the number of months with less than 100 mm precipitation. Extended measurements during LBA at Santarem (Goulden et al. 2004; da Rocha et al. 2004; Miller et al. 2004), which has a longer 4-month dry season gave a much more detailed picture. Da Rocha et al. (2004) showed that ET in fact increased from 3.18 $\pm$ 0.76 mm/d during the wet season to 3.96 $\pm$ 0.65 mm/d during the dry season, as net radiation, Rn, and water vapor deficit increased. For this site near $-3°$S, the annual cycle of Rn is dominated by the annual cycle of cloud cover (see section 4.5). Clearly the lack of drought stress during the dry season is a consequence of deep rooting and probably vertical water movement within the soil. NEE measurements from the same forest showed a loss of carbon in the wet season and a gain in the dry season (Saleski et al. 2003) with a net annual loss. This was surprising at the time, as it was the reverse of the seasonal cycle of NEE in many models. It has prompted the development of new model parameterizations (see section 4.4).

4.2 Role of deep rooting and soil water transports

The deep rooting in tropical forests is fundamental to their existence (Nepstadt et al. 1994). In addition, hydraulic redistribution of soil water by roots at night, upward in the dry season and downward in the wet season, plays an important role in increasing the water available to the forest (da Rocha et al. 2004; Oliveira et al. 2005); both in the dry season and during periods of drought (Saleska et al. 2007).

Bruno et al. (2006) used frequency-domain reflectometry to make continuous, high-resolution measurements for 22 months of the soil moisture to a depth of 10 m in the Amazonian rain forest at Santarem, where the mean annual precipitation is over 1900 mm. In the 4-month dry season, ET is about 150 mm mo^{-1}, much higher than precipitation, which averages about 60 mm mo^{-1}. The soil field capacity was approximately 0·53 m^3 m^{-3} and was nearly uniform with soil depth. Soil moisture decreased at all levels during the dry season, with the minimum of 0·38 m^3 m^{-3} at 3 m beneath the surface. They confirmed that the zone of active water withdrawal extended to a depth of at least 10 m. They also found that moisture withdrawal from the upper 10 m of soil during rain-free periods agreed well on a daily basis with ET measurements made by the eddy covariance technique. However, the upper 2 m of soil supplied 56% of the water used for ET in the wet season, but only 28% of the water used for ET in the dry season. They observed an increase of soil moisture at night at a depth of 0.6 m in all seasons, suggesting an upward transport though the one-meter level. Thus, the forest at the site was well adapted to the normal cycle of wet and dry seasons; and the dry season had only a small effect on ET, because of the very large available water storage.

4.3 Aerosol enhancement of NEE by diffuse light

Studies have shown for some time that diffuse radiation, scattered either by clouds or aerosols, increases carbon uptake by forests (Gu et al. 1999, 2002, 2003; Niyogi et al. 2004). We will not address the scattering by clouds here, but Oliveira et al. (2007) confirmed the enhancement of NEE by aerosol scattering for two LBA sites: one south of Santarém and one at the Jaru forest in Rondônia. They measured aerosol optical thickness (AOT) with sun photometers, and CO_2 uptake by eddy-correlation. They found that for small AOT $\approx$ 1.6, NEE had a maximum enhancement of 11% for the Santarém site and 18% for the Jaru forest. Only at large AOT $>$ 2.7 was NEE reduced by the reduction in total solar radiation. Considering that aerosols from biomass burning are present in most tropical areas in the dry season, with AOT in the range $<$2 over wide regions, this is clearly a climate coupling of significance to models. It is also one of the mechanisms, in addition to the impact of much reduced cloudiness on incoming solar radiation, which gives the NEE maximum in the dry season, noted in section 4.1.

4.4 Reconciliation of NEE observations and land-surface models

Biogeophysical land-surface models have had difficulty reproducing the annual cycle of NEE in some regions of the Amazon; generally simulating uptake of carbon during the wet season and loss of carbon during seasonal drought, whereas in reality the opposite occurs (Saleski et al. 2003). Since NEE is the difference of photosynthetic uptake and respiration loss, the wrong sign of the annual cycle may well involve errors in both. For example, if deep rooting and hydraulic recharge reduce soil water stress, then a higher photosynthetic uptake in the dry season is likely, because reduced cloud increases light levels and aerosols increase diffuse radiation. There is also evidence of reduced near-surface root respiration in the dry season (Goulden et al. 2004).

Baker et al. (2008) introduced a series of mechanisms into the third version of the Simple Biosphere model (SiB3), and were successful in reversing the annual cycle of NEE to match the observations for the forest south of Santarém. Increases in soil storage and root uptake were needed, as discussed in section 4.2. They introduced a 10 m soil depth, introduced the movement of water in the soil via hydraulic redistribution to allow for more efficient uptake of water in the soil layer during the wet season and the moistening of near-surface soil during the annual drought. They relaxed the soil water stress function, changing it from a direct coupling to root fraction in each soil layer to a coupling to plant available water within the total column, independent of root distribution. They then allowed extraction of soil water based on actual root fraction and moisture content of the layer. Collectively these changes reduced water stress during the dry season. An important change was made to the optimum soil moisture for respiration, which reduced soil respiration in the dry season, consistent with observations.

A separate canopy modification was introduced to increase the photosynthetic response to elevated light levels during the dry season. This involved a modification of two-stream canopy radiative transfer sub-model and the canopy photosynthesis treatment to accommodate sunlit and shaded canopy fractions in the prognostic canopy air space (Baker et al. 2008).

These changes are illustrative of the challenge of modeling complex ecosystems using simplified biophysical models (SiB3 maintains, for example, a constant annual leaf area index for broadleaf evergreen forests). Observational studies have driven the introduction of more realistic soil water

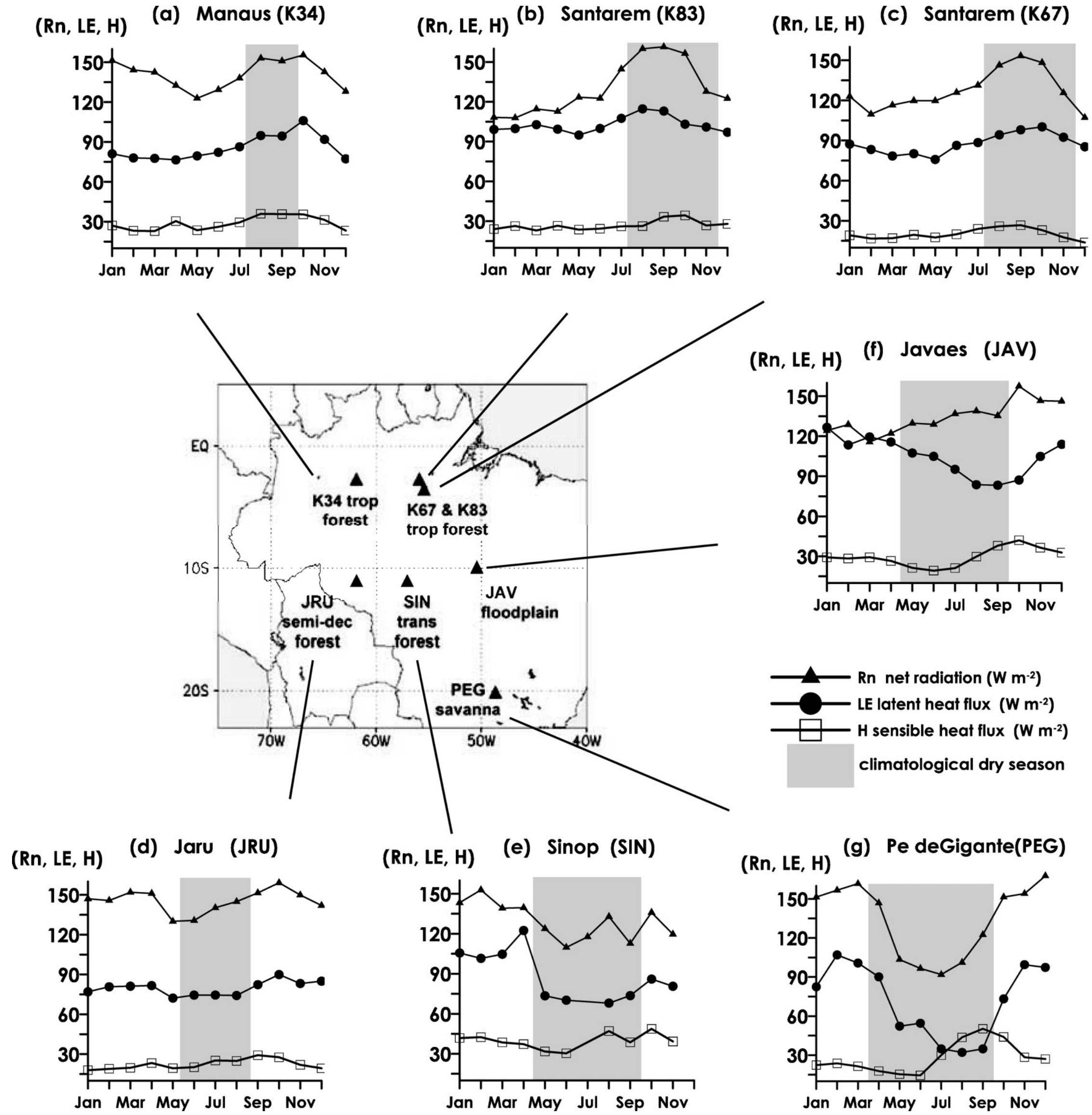

Figure 6. Mean monthly latent heat flux (LE), net radiation (Rn) and sensible heat flux (H) in Wm^{-2} for (a) K34, (b) K83, (c) K67, (d) JRU, (e) SIN, (f) JAV and (g) PEG. The climatological dry season is shaded (from da Rocha et al. 2009a).

reservoirs and improved rooting models, but the parameterizations of the dependence of soil respiration to temperature and moisture remain critical components in the net ecosystem exchange. In addition the coupling between photosynthesis and direct and diffuse radiation is complex for forest canopies; and the control on the radiation field by clouds and aerosols involves direct coupling between ET and surface fires, BL processes and convection.

4.5 The biome gradient: forest to savannah

A central objective of LBA was to understand the transition in the surface exchanges across the biome gradient from forest to savannah in the present climate. Da Rocha et al. (2009a) analyzed data from the LBA network of flux tower sites, included tropical humid and semi-deciduous forest, transitional forest, floodplain and *cerrado.* Figure 6 is a reproduction of their Figure 2, showing the seasonal cycle of Rn, LE and H for seven flux sites at three different latitude bands (roughly -3, -10 and -21°S) at the locations shown in the inset map. They note that although the small sensible heat flux, H, typically increases slightly in the dry season, the controls on evapotranspiration seasonality changed along the biome gradient, with net radiation playing a more important role in the wetter forests, and soil moisture playing a more important role in the drier savannah sites towards the south-east. They found that at sites with an annual precipitation above 1900 mm and a dry season length less than 4 months (Manaus, Santarém and Jaru in Rondônia), evaporation rates increased in the dry season,

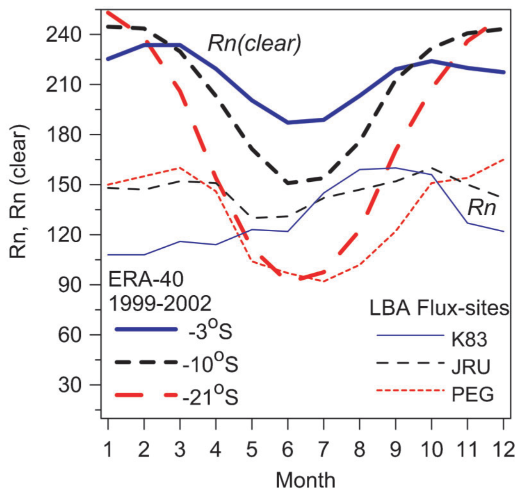

Figure 7. Latitudinal gradient of Rn(clear) from ERA-40 (heavy lines) and Rn (light lines) from the corresponding flux sites, K83, JRU, and PEG from Figure 6.

coincident with increased radiation. In contrast, ecosystems with precipitation less than 1700 mm and a longer dry season (Sinop, Javaes and Pe deGigante) showed clear evidence of reduced evaporation in the dry season. There is a N-S latitudinal variation of the clear-sky flux Rn(clear), and this is strongly modulated by the seasonal variation of cloud cover across the Amazon to give the Rn that drives the surface energy balance.

Figure 7 compares Rn from Figure 6 for three sites across the biome, K83, JRU and PEG (light curves), with the corresponding Rn(clear) (heavy curves) taken from the ERA-40 reanalysis for the nearest gridpoints to K83, JRU and PEG. These are clear-sky averages from January 1999 to August 2002, when ERA-40 ended. The interannual variation on the monthly timescale is small. The seasonal variation of Rn(clear) increases with latitude and is largest for PEG at $-21°$S.

Because SWCF + LWCF is dominated by the SWCF, which is negative, Rn $<$ Rn(clear) in the tropics, and the separation is a measure of cloud cover (see below). For June at PEG (in the dry season) computed Rn(clear) $<$ Rn from the data, indicating a small incompatibility between model calculation and observations. The reanalysis Rn(clear) could be too low if the model surface albedo, 0.15 in June for the PEG gridpoint, is too high, or because of biases in the atmospheric temperature and moisture structure. Alternatively these Rn observations could have a small high bias. Note that as in section 3.3, we use ERA-40 for clear-sky net radiation, because the ERA-Interim values are well below the corresponding observations in nearly clear-sky conditions at PEG in the dry season.

The total cloud forcing

$$CF = SWCF + LWCF = Rn - Rn(clear) \qquad (6)$$

Using (2) and approximation (5) gives

$$\begin{aligned} Rn - Rn(clear) &\approx \alpha_{cloud}(SW_{net}(clear) + LW_{net}(clear)/1.3) \\ &\approx \alpha_{cloud}Rn(clear) \end{aligned} \qquad (7)$$

if we further neglect the factor of 1.3 in the second smaller term. Thus the vertical separation between Rn and Rn(clear) in Figure 7, scaled by Rn(clear), is an approximate measure of the effective cloud albedo (ignoring also the uncertainty in the cross-calibration of the reanalysis clear-sky computations and the flux-site observations).

The effective cloud albedo falls from about 50% in the wet season to about 20% in the dry season at K-83 south of Santarem. The seasonal cycle of Rn is dominated by the change in cloud cover, not the seasonal cycle of Rn(clear). The same is true at Jaru in Rondônia, where the change in cloud cover, from about 40% in the wet season to about 15% in the dry season, almost removes the substantial seasonal variation in the clear sky net flux. Even at PEG, the seasonal variation of cloud cover, from about 35% in the wet season to near zero in the dry season, is sufficient to reduce the seasonal amplitude of Rn to less than half the clear-sky variation (which at $-21°$S is dominated by the large variation in solar zenith angle).

Since BL cloud cover is tightly coupled locally to the sub-cloud layer in the daytime in the tropics, and much of the middle and high-level cloud also originates from convection which is coupled to the BL; it is clear that the surface energy balance and the cloud field form a tightly coupled system over Amazônia on diurnal time-scales and space-scales of order a few hundred km. Historically, Rn has been treated as 'external' to the surface energy balance; as one component driving 'evaporative demand'. But it is clear from LBA that this is not a useful concept for understanding the equilibrium climate of a system in which surface biogeochemistry, BL processes, aerosols and the cloud field are so tightly coupled on the diurnal timescale. The difficulty of modeling this fully coupled system remains one of the major sources of uncertainty in our climate models. We have of course not addressed here the impact of deforestation on the local regional and global climate (Silva Dias et al. 2009).

4.6 Role of ET in wet season onset

Surface and BL processes and precipitation drive the regional-scale circulation. Fu and Li (2007) discuss the influence of the land surface on the transition from dry to wet season in Amazônia. Their analysis of fifteen years of ERA-40 data suggests that the transition from dry to wet season in Southern Amazônia is initially driven by increases of surface latent heat flux, which increases Convective Available Potential Energy (CAPE) and provides favorable conditions for increased rainfall even before the large-scale circulation has changed. They suggest that the increased diabatic heating initiates the reversal of the cross-equatorial flow, leading to large-scale net moisture convergence over Southern Amazônia. They found that if the dry season was long with low rainfall, the reduced surface latent heat flux leads to a delay in the onset of the wet season. From this they infer that any land use change in Amazônia that reduces rainfall during the dry and transition seasons could significantly delay the wet season onset and so prolong the dry season.

It should be noted that the seasonal cycle of evaporation in ERA-40 is too large because the model has insufficient moisture storage in the model root-zone, and this could influence their results. Nonetheless their discussion is relevant to the question of whether the large-scale circulation over the Amazon may be affected by climate change, if there is a substantial transition from forest to grassland, which would introduce a larger seasonal cycle.

5. Aerosol effects: radiation and cloud microphysics

Progress in aerosol research has been rapid during the course of LBA. When Figure 1 was drafted, the only role given to aerosols was their impact on the surface radiation budget, and at that time global aerosol analyses were not yet routinely available. Over the Amazon, the extensive burning of agricultural land and forests in the dry season impacts not only the radiative budget of the surface and atmosphere, but also the surface NEE (through the scattering of light) and the microphysics of clouds and precipitation. Many papers have reviewed basic aerosol processes over the Amazon (Artaxo et al. 2002; Andreae et al. 2002) and their impact of aerosols on clouds and precipitation (Andreae et al. 2004; Andreae and Rosenfeld, 2008).

On the global scale, near-real-time analyses and forecasts are now available from ECMWF for five classes of aerosols, using available global datasets (Benedetti et al. 2009; Morcrette et al. 2009), as part of the Global Earth-system Monitoring using Space and in-situ data - the GEMS project. Figure 8 shows ECMWF monthly analyses of aerosol optical depth for September 2003 and 2004 over S. America, produced by GEMS. There are extended areas with AOT ≈ 1 or greater; in the range where aerosol scattering enhances NEE, as discussed in section 4.3. The interannual difference is clearly visible. These ECMWF aerosol analyses depend critically on satellite aerosol optical depth observations at 550 nm, as the aerosol transport model does yet include a process that is important over the Amazon; the enhanced vertical transport of aerosols by convective plumes driven by fires. The operational Brazilian forecast system for aerosol and pollutant transport based on LBA research is discussed in section 5.1.

It is a challenge to define source terms for the many different types of aerosols, as well as their subsequent atmospheric transport and chemistry. In the next few sections, we will review some selected topics that are particularly important in South America: the computation of emissions from fires; the role of the plume rise of vegetation fires on vertical transports in the atmosphere, aerosol-cloud-precipitation coupling during the transition between dry and wet seasons and briefly the possible radiative impact of smoke aerosol on the monsoon transition.

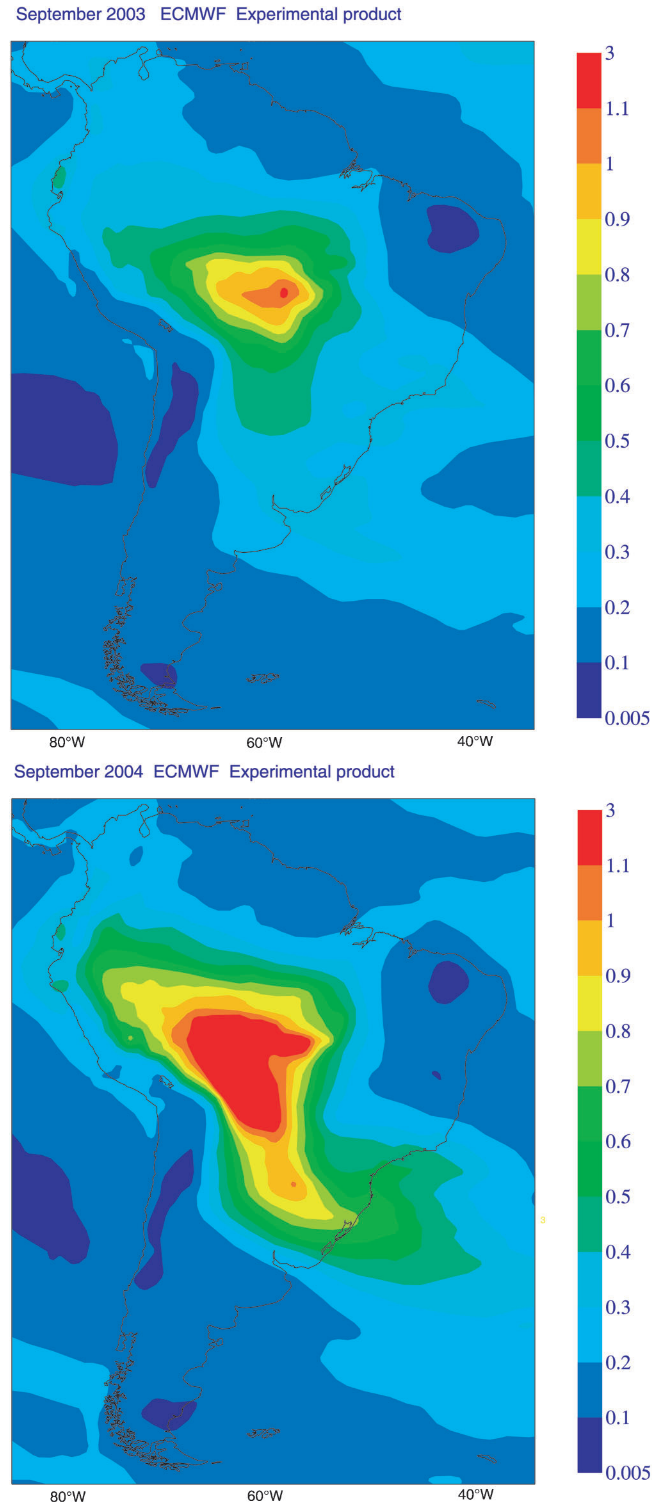

Figure 8. GEMS ECMWF analyses of aerosol optical thickness for (upper) September, 2003 and (lower) September 2004. (Morcrette, 2009, personal communication)

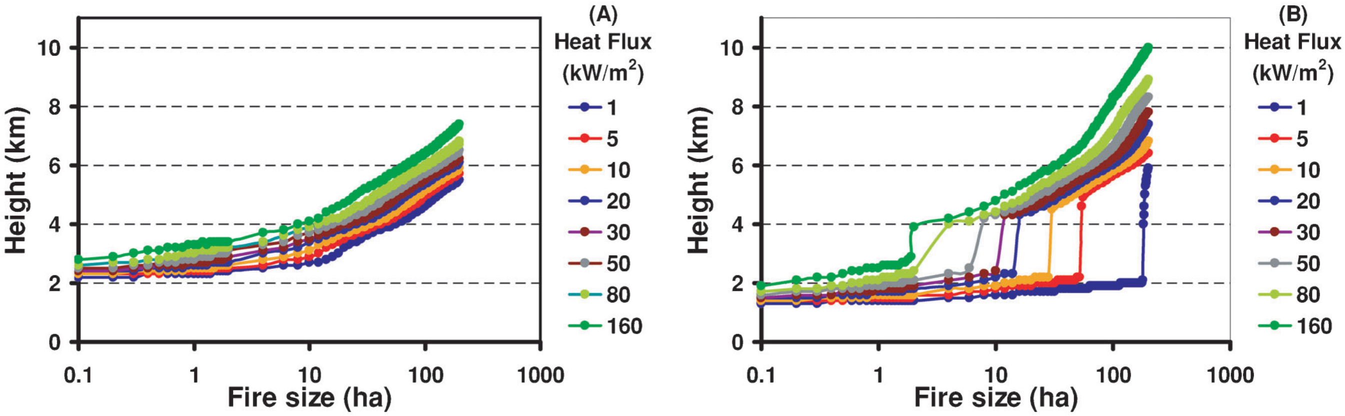

Figure 9. Simulated fire plume rise as a function of fire size and heat flux in (left) stable and (right) moist unstable atmospheric regimes (from Freitas et al. 2007).

5.1 Real-time modeling of aerosol from biomass burning.

A Coupled Aerosol and Tracer Transport model for the Brazilian Regional Atmospheric Modeling System (CATT-BRAMS) (Freitas et al. 2009; Longo et al. 2007) was developed to address the real-time modeling of the aerosol source from biomass burning. This operational Brazilian forecast system, which incorporates LBA research on aerosols, can be found at http://meioambiente.cptec.inpe.br/.

The biomass burning emission parameterization is an extension of Freitas et al. (2005). For each fire pixel detected, the mass of the emitted tracer is calculated by the following expression

$$M_{[\eta]} = \alpha_{veg} \ \ \beta_{veg} \ . \ Ef_{veg}^{[\eta]} \ \ a_{fire} \qquad (8)$$

where α_{veg} is the estimated value of the above-ground biomass available for burning (in kg m^{-2}), coming from a carbon-density map, β_{veg} is a combustion factor, $Ef^{[\eta]}{}_{veg}$ is an emission factor for a species [η], and a_{fire} is the burning area for each burning event. For example, for the three biome categories of (tropical forest, savanna, pasture), the respective fraction $\beta_{veg} = (0.48, 0.78, 1.0)$; while the corresponding emission factors for CO are (110, 63, 49) g kg^{-1}, and for particulate pollution (PM2.5), they are (8.3, 4.4, 2.1) g kg^{-1}.

To minimize missing remote observations, the burning area is a hybrid product derived from three sources: the Geostationary Operational Environmental Satellite-Wildfire Automated Biomass Burning Algorithm (GOES-WFABBA product (http://cimss.ssec.wisc.edu/goes/burn/wfabba.html, Prins et al. (1998); the Brazilian National Institute for Space Research fire product, which is based on the Advanced Very High Resolution Radiometer (AVHRR) aboard the NOAA polar orbiting satellites (http://www.cptec.inpe.br/queimadas, Setzer and Pereira 1991) and the Moderate Resolution Imaging Spectroradiometer (MODIS) fire product (http://modis-fire.umd.edu, Giglio et al. 2003).

5.2 Plume Rise of Vegetation Fires

Vegetation fires play a significant role in vertical transport over Amazônia, where the atmosphere is conditionally unstable. This sub-grid-scale process is not resolved in typical forecast models with grid resolutions of order 25–50 km, nor is it included in conventional convective parameterizations. However, given a fire data-base, the transports driven by plume rise can also be parameterized. Freitas et al. (2006, 2007, 2009) describe such a parameterization to include the vertical transport of hot gases and particles emitted from biomass burning in low resolution atmospheric chemistry transport models. The mechanism is to embed a 1-D cloud-resolving model with appropriate lower boundary conditions in each column of the 3-D host model.

Figure 9 shows the sensitivity of the model plume rise to the surface forcing, represented by fire size and heat flux, and the atmospheric stability. The left panel is a 'dry, stable' case with a strong thermal inversion around 800 hPa and a very dry layer above, and the right panel shows the greater plume rise in a moist unstable case, where there is a weaker thermal inversion around 870 hPa and a much moister layer above. Larger fires, typical of the dry season over Amazônia, transport pollutants, aerosols and water out of the boundary layer into the middle and upper troposphere.

Freitas et al. (2007) show that the fire size distribution is broad: with fire frequency decreasing with fire size, and 75% of detected fires having a size below 20 ha. Heat fluxes from forest fires typically range from 30–80 kW m^{-2}, while for savannah fires the heat fluxes are smaller in the range 4–23 kWm^{-2}

5.3 Impact of forest fires plume rise on mid-tropospheric dispersion

Dispersion in the free troposphere depends on the level at which pollutants are injected by fires. Freitas et al. (2006) put this 1-D plume model, coupled to the fire emission model, into the 3-D CATT-BRAMS, and found more

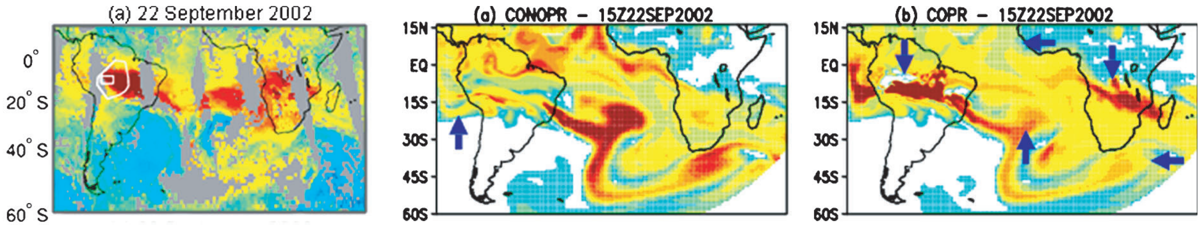

Figure 10. Comparison of mid-tropospheric dispersion of CO in AIRS observation (left) with CATT-RAMS, without plume rise model (center) and with 1-D plume-rise sub-grid model (right) (from Freitas et al. 2006).

realistic dispersion of carbon monoxide (CO) in the middle troposphere. Figure 10, a case study for 22 September, 2002, compares 500 hPa retrievals of CO from the Atmospheric Infrared Sounder (AIRS) with the dispersion of CO at 5.9 km altitude in the model, both with (labeled COPR) and without (CONOPR) the insertion of the sub-grid-scale plume rise model. The arrows mark where a model simulation is better. The agreement is generally better with the plume rise model on the right (COPR), although differences remain.

5.4 Aerosol-cloud-precipitation coupling

Amazônia is remarkable for the wide range of convective regimes both across the region and during the annual cycle. The large variability in atmospheric aerosol impacts both cloud microphysics and cloud electrification, although circulation changes also affect convective organization (Herdies et al. 2002; Rickenbach et al. 2002). In Rondônia in the south-western Amazon, convection in the rainy season in low-level westerly flows with low aerosol content resembles oceanic convection with precipitation from warm rain processes and little electrification (Williams et al. 2002). At the other extreme in the dry season in Rondônia, widespread fires produce a high aerosol loading with high numbers of cloud condensation nuclei from biomass burning (Martins et al. 2009b). Convection is then dominated by ice-phase processes with frequent lightning and deep clouds with convective tops in the lower stratosphere (Williams et al. 2002; Fuzzi et al. 2007).

Measurements of cloud condensation nuclei (CCN) and cloud size distribution properties taken in the southwestern Amazon region during the transition from dry to wet seasons (Andreae et al. 2004; Gonçalves et al. 2008; Martins and Silva Dias, 2009) clarify the differences in the droplet distributions. Increased pollution and more CCN have two important impacts. Firstly, polluted conditions give high concentrations of cloud droplets with smaller effective radius, because the liquid water content during polluted periods was similar to that in clean periods. Secondly, in polluted periods the relative dispersion of the droplet distributions decreases. Both these changes greatly reduce the growth of droplets by warm rain processes, so cloud microphysics in polluted conditions become dominated by ice-phase processes (Andreae et al. 2004; Freud et al. 2008).

Recently nested modeling simulations using BRAMS have successfully showed the fundamental link between cloud droplet spectra, convective structure and precipitation (Martins et al. 2009a). Gonçalves et al. (2008) and Martins and Silva Dias (2009) were used as guidelines to define the microphysical shape parameters for the simulations in the BRAMS model. Figure 11 from Martins et al. (2009a) shows the vertical structure of cloud and ice water mixing ratio observed at the time of maximum liquid water path for a sequence of simulations for increasing CCN concentrations: 300 cm^{-3}, 450 cm^{-3}, 600 cm^{-3}, and 900 cm^{-3}; with corresponding values of 3, 4, 5, 6 specified for the shape parameters for the cloud droplet gamma distributions. With increasing CCN concentrations, cloud droplet number, maximum updraft speeds, peak rainfall rates, ice concentrations and cloud top heights all increased. There was a change from a warm to a cold rain process. Locally, convective cells became deeper and more intense, increasing both maximum precipitation and giving higher peaks in the accumulated precipitation. However, total precipitation, spatially and temporally averaged over the domain, showed no systematic trend with CCN concentrations.

There were some secondary radiative feedbacks. Under polluted conditions, mean cloud cover diminished, allowing greater amounts of solar radiation to reach the surface. Including the effects of aerosol absorption of radiation in the lower layers of the atmosphere delayed convective evolution, increasing instability and yielding slightly higher maximum rainfall rates.

Lin et al. (2006) presented the empirical relationships between aerosol- and precipitation-related parameters, based on satellite data from the MODIS and Tropical Rainfall Measuring Mission instruments. The authors showed that, during the transition from the dry to wet season in two different years, an increase in aerosol concentration was associated with a change in the probability density function of rainfall rates: increasing the number of events presenting higher rainfall rates, as well as increasing the water paths (liquid and ice), increasing high-level cloud cover and decreasing cloud top temperatures. Koren et al. (2008) discuss in a broader sense, also with data from satellites, how in the Amazon basin two opposing effects

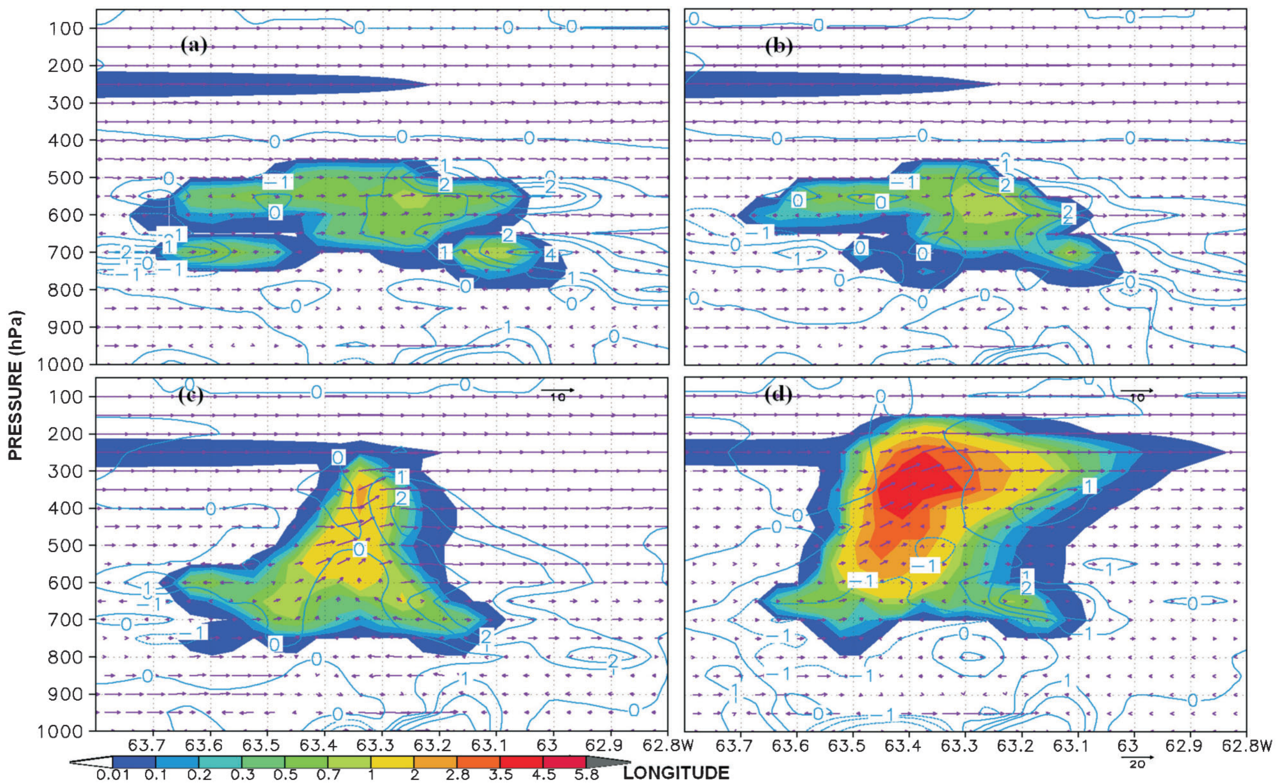

Figure 11. Vertical structure of cloud and ice water mixing ratio (g/kg) observed at the time of maximum liquid water path for a typical convective cell for scenarios with increasing CCN (a) 300, (b) 450, (c) 600 and (d) 900 cm^{-3}. Contour lines represent the vapor mixing ratio temporal evolution (g/kg/h) (from Martins et al. 2009a).

control the aerosol precipitation interaction, the radiative and the microphysical, leading to either suppression (see numerical experiments by Vendrasco et al. 2009 for the eastern Amazon region), or enhancement of convective development as discussed above.

5.5 Aerosol-Circulation coupling

Zhang et al. (2009) address the larger-scale issue of the impact of aerosol from extensive biomass burning on the monsoon circulation transition over Amazônia. They found, using a regional climate model, that aerosol radiative forcing from strongly absorbing smoke aerosols warm and stabilize the lower troposphere and increase the surface pressure within the smoke center in southern Amazônia. This weakens the southward surface pressure gradient between northern and southern Amazônia, and induces an anomalous moisture divergence in the smoke center. They suggest this inhibits the northward propagation of synoptic cyclonic disturbances from extratropical South America.

6. Conclusions

We have reviewed progress in understanding land-surface-atmosphere coupling over the Amazon that has come from LBA research. We started by updating a diagram from Betts et al. (1996) of the coupling between land and atmosphere. New links were added to show the role of clouds and aerosols in the radiative budget from a surface climate perspective; the impact of diffuse radiation from aerosols and clouds and deep rooting on NEE; the impact of surface emissions and aerosols on the microphysics of clouds and precipitation; the role of convection in the vertical transport of atmospheric species, the coupling between clouds, mesoscale dynamics and atmospheric structure and land-use and land-cover. We chose a subset of these topics for discussion in this paper.

We then discussed the reformulation of cloud forcing in the surface energy budget in terms of an effective cloud albedo (per unit area of surface); a concept that emerged from land-surface studies of the Amazon using ERA-40 reanalysis data. The concept was then used to compare the effective cloud albedos derived from measured SW_{down} fluxes at two sites in Rondônia: the Jaru forest site and FNS pasture site. The pasture site has a 6% higher effective cloud albedo in July as well as an 8% higher surface albedo, which together give a substantial reduction in net radiation of about 14%. Using data from these same two Rondônia sites, we showed how the diurnal temperature range has a quasi-linear relation to the daily mean longwave cooling; and the net longwave flux is a function largely of near-surface RH and effective cloud albedo. As a result, the longwave cloud forcing can be approximated in terms of this effective cloud albedo and the clear-sky longwave flux, and the diurnal temperature range has a nearly linear relation to effective cloud albedo. The picture that emerges is one of tight coupling between the near-surface climate, the boundary layer and the cloud field which has roots in the sub-cloud layer. Convection and clouds over the Amazon are almost always coupled to the subcloud layer in the daytime, which means that, on daily timescales, the SWCF and LWCF, the surface energy budget, the near-surface climate, the diurnal temperature range, cloud-base and the BL equilibrium together form a tightly coupled system, which responds to the atmospheric forcing of mean ascent or descent on regional scales.

The seasonal cycle of an old-growth forest showed an increase in ET and NEE in the dry season, which was inconsistent with many early model studies. However it is clear that the deep forest rooting systems make water available throughout the year, whereas in the dry season the SWCF is reduced by regional scale subsidence, so that more light is available for photosynthesis. The aerosol optical thickness also increases in the dry season, and studies of two Amazon forest canopies show that for AOT $\approx$ 1.6, diffuse light scattered by aerosols increases NEE by 11–18%.

We discussed the substantial changes in a SiB-3 land-surface model needed to reproduce the observed annual cycle of NEE, which is positive in the dry season and negative in the wet season for the old-growth forest south of Santarém. Many changes in the soil rooting and hydrology were necessary to reduce water stress during the dry season: a 10 m soil depth to give a larger reservoir; hydraulic redistribution to allow for more efficient uptake of water during the wet season and the moistening of near-surface soil during the annual drought, and a new soil water stress function coupled to plant available water within the total column, independent of root distribution. In addition, a change in the optimum soil moisture for respiration was needed to reduce soil respiration in the dry season; and the canopy model was modified to increase the photosynthetic response to elevated light levels during the dry season. This illustrate the paramount need for high quality observations to identify errors in model representation of processes, but also the challenge of modeling complex biological ecosystems.

The network of LBA sites, which includes tropical humid and semi-deciduous forest, transitional forest, floodplain and *cerrado,* has improved our understanding of the biome gradient across the Amazon. At sites with an annual precipitation above 1900 mm and a dry season length less than 4 months (Manaus, Santarem and Jaru in Rondônia), evaporation rates increased in the dry season, coincident with increased radiation (da Rocha et al. 2009a). In contrast, ecosystems with precipitation less than 1700 mm and a longer dry season (Sinop, Javaes and Pe deGigante) showed clear evidence of reduced evaporation in the dry season coming from soil water stress. In all these sites the seasonal variation of the 'effective cloud albedo' is a major factor in determining the surface available energy.

Aerosol research in LBA has been central to progress in understanding land-atmosphere coupling: we addressed only a small subset of issues. Dry season fires add substantial aerosol to the atmosphere. Aerosol scattering and absorption both reduce the total downward surface radiative flux, but the diffuse/direct flux ratio is increased and this can increase NEE for low AOT, as discussed above. Global aerosol analyses have reached operational status but more detailed physical parameterizations are needed. For example, the sub-grid-scale vertical transport of aerosols over the Amazon is enhanced by convective plumes produced by fires. In moist unstable regimes, fires can effectively inject smoke aerosol and gases directly into the middle troposphere with substantial impacts on mid-tropospheric dispersion.

Progress has been also been made in understanding and modeling aerosol-cloud-precipitation coupling. In the rainy season in Rondônia, convection in low-level westerly flows with low aerosol content resembles oceanic convection with precipitation from warm rain processes and little electrification. But in the same region in the dry season, widespread fires produce a high aerosol loading with high numbers of cloud condensation nuclei from biomass burning; and convection is then dominated by ice-phase processes giving deep clouds with frequent lightning and convective tops in the lower stratosphere. Recent studies based on measurements of CCN and cloud droplet distributions have successfully modeled this wide range of convective regimes and shown the fundamental link between cloud droplet spectra, convective structure and precipitation. However, the parameterization of these aerosol-precipitation interactions in climate models remains a challenge.

Uncovering the critical links between surface, BL processes and precipitation and the regional scale circulation is more difficult, and we have touched on only a couple of topics. One study with ERA-40 data suggests that the transition from dry to wet season in Southern Amazônia is initially driven by increases of surface latent heat flux, which increases CAPE and increases rainfall even before the large-scale circulation has changed. This study showed that if the dry season was long with low rainfall, the reduced surface latent heat flux led to a delay in the onset of the wet season. From this they inferred that any land use change in Amazônia that reduces rainfall during the dry and transition seasons could significantly delay the wet season onset and prolong the dry season. Another study found that aerosol radiative forcing from strongly absorbing smoke aerosols warms and stabilizes the lower troposphere and induces an anomalous moisture divergence in the smoke center, which inhibits the northward propagation of synoptic cyclonic disturbances from extratropical South America, and delays the monsoon circulation transition over Amazônia.

Much progress has been made in understanding the details of processes and their interactions. Nonetheless, accurate representation of the coupling between clouds, aerosols and the surface energy balance, the diurnal cycle of convection, and the coupling between aerosols, convective precipitation, the large-scale circulation and the climate still present substantial modeling challenges, because our reductionist approach to modeling the earth system faces a fundamental difficulty. We have to identify important processes before they can be introduced into models in the form of detailed sub-models and parameterizations. This increases complexity, and the overall behavior of the fully coupled system depends on modeling correctly all the feedback loops. LBA has once again shown how field observations of the behavior of the coupled system on different time and space-scales are essential for the development and testing of realistic models.

Acknowledgements: Alan Betts acknowledges support from the National Science Foundation, under Grant AGS-0529797. Maria Assunção F. da Silva Dias acknowledges the support of Conselho Nacional de Desenvolvimento Científico e Tecnológico through their Research Grant (PQ). FAPESP and MCT/Milênio also funded part of the LBA research. We deeply appreciate the collaboration of so many scientists from around the world who have contributed to the success of the Large Scale Biosphere-Atmosphere Experiment in Amazônia.

References

Andreae, M.O., P. Artaxo, C. Brandão *et al.*, 2002: Biogeochemical cycling of carbon, water, energy, trace gases and aerosols in Amazonia: The LBA-EUSTACH experiments. *J. Geophys. Res.*, **107**, 8066, doi: 10.1029/2001JD000524.

Andreae, M.O., D. Rosenfeld, P. Artaxo, A.A. Costa, G.P. Frank, K.M. Longo and M.A.F. Silva-Dias, 2004: Smoking rain clouds over the Amazon. *Science*, **303**, 1337–1342, doi: 10.1126/science.1092779.

Andreae, M.O. and D. Rosenfeld, 2008: Aerosol–cloud–precipitation interactions. Part 1. The nature and sources of cloud-active aerosols. *Earth-Science Reviews*, **89**, 13–41, doi: 10.1016/j.earscirev.2008.03.001.

Artaxo, P., J.V. Martins, M.A. Yamasoe, A.S. Procópio, T.M. Pauliquevis, M.O. Andreae, P. Guyon, L.V. Gatti, and A.M.C. Leal, 2002: Physical and chemical properties of aerosols in the wet and dry season in Rondonia, Amazonia. *J. Geophys. Res.*, **107**, 8081, doi: 10.1029/2001JD000666.

Baker, I. T., L. Prihodko, A. S. Denning, M. Goulden, S. Miller, and H. R. da Rocha, 2008: Seasonal drought stress in the Amazon: Reconciling models and observations, *J. Geophys. Res.*, **113**, G00B01, doi: 10.1029/2007JG000644.

Benedetti, A., J.-J. Morcrette, O. Boucher, A. Dethof, R.J. Engelen, M. Fisher, H. Flentje, N. Huneeus, L. Jones, J.W. Kaiser, S. Kinne, A. Mangold, M. Razinger, A.J. Simmons, M. Suttie, and the GEMS-AER team, 2009: Aerosol analysis and forecast in the ECMWF Integrated Forecast System: Data assimilation. *J. Geophys. Res.*, **114**, D13205, doi: 10.1029/2008JD011115.

Betts, A.K., 2004: Understanding Hydrometeorology using global models. *Bull. Amer. Meteorol. Soc.*, **85**, 1673–1688, doi: 10.1175/BAMS-85-11-1673.

Betts, A.K., 2006: Radiative scaling of the nocturnal boundary layer and the diurnal temperature range. *J. Geophys. Res.*, **111**, D07105, doi: 10.1029/2005JD006560.

Betts, A.K., 2009: Land-surface-atmosphere coupling in observations and models. *J. Adv. Model Earth Syst., Vol. 1, Art. #4,* 18 pp., doi: 10.3894/JAMES.2009.1.4.

Betts, A.K., J.H. Ball, A.C.M. Beljaars, M.J. Miller and P. Viterbo, 1996: The land-surface-atmosphere interaction: a review based on observational and global modeling perspectives. *J. Geophys. Res.* **101**, 7209–7225, doi: 10.1029/95JD02135.

Betts, A.K and P. Viterbo, 2005: Land-surface, boundary layer and cloud-field coupling over the south-western Amazon in ERA-40. *J. Geophys. Res.*, **110**, D14108, doi: 10.1029/2004JD005702.

Betts, A.K., J. Ball, A. Barr, T. A. Black, J. H. McCaughey and P. Viterbo, 2006: Assessing land-surface-atmosphere coupling in the ERA-40 reanalysis with boreal forest data. *Agricultural and Forest Meteorology*, **140**, 355–382, doi: 10.1016/j.agrformet.2006.08.009.

Betts, A. K., M. Köhler, and Y. Zhang, 2009a: Comparison of river basin hydrometeorology in ERA-Interim and ERA-40 reanalyses with observations. *J. Geophys. Res.*, **114**, D02101, doi: 10.1029/2008JD010761.

Betts, A.K., M.A.F. Silva Dias, G. Fisch, C. von Randow, J.C.P. Cohen, R. da Silva, D.R. Fitzjarrald, 2009b: The Amazonian Boundary layer and mesoscale circulations. IGBP Synthesis Vol. *Amazonia and Global Change*. Eds. M. Keller, J. Gash, P. Silva Dias. *Geophys. Monograph Ser.*, **186**.

Betts, R., P. Cox, M. Collins, P. Harris, C. Huntingford, and C. Jones, 2004: The role of ecosystem-atmosphere interactions in simulated Amazonian precipitation decrease and forest die-back under global change warming. *Theor. Appl. Climatol.*, **78**, 157–175, doi: 10.1007/s00704-004-0050-y.

Bruno, R.D., H.R. da Rocha, H.C. de Freitas, M.L. Goulden and S.D. Miller, 2006: Soil moisture dynamics in an eastern Amazonian tropical forest. *Hydrol. Process.*, **20**, 2477–2489, doi: 10.1002/hyp.6211.

Cox, P., R. Betts, M. Collins, P. Harris, C. Huntingford and C. Jones, 2004: Amazonian forest dieback under climate-carbon cycle projections for the 21st century. *Theor. Appl. Climatol.*, **78**, 137–156, doi: 10.1007/s00704-004-0049-4.

Cutrim, E., D.W. Martin, and R. Rabin, 1995: Enhancement of cumulus clouds over deforested lands in

Amazonia. *Bull. Amer. Meteor. Soc.*, **76**, 1801–1805, doi: 10.1175/1520-0477(1995)076<1801:EOCCOD>2.0.CO;2.

da Rocha, H.R., M.L. Goulden, S.D. Miller, M.C. Menton, L.D.V.O. Pinto, H.C.F. de Freitas and A. M. e Silva Figueira, 2004: Seasonality of water and heat fluxes over a tropical forest in eastern Amazônia. *Ecol. Appl.*, **14**(4), supplement, S22–S32, doi: 10.1890/02-6001.

da Rocha, H. R. and 18 co-authors, 2009a: Patterns of water and heat flux across a biome gradient from tropical forest to savanna in Brazil. *J. Geophys. Res.*, **114**, G00B12, doi: 10.1029/2007JG000640.

da Rocha, H.R., A.O. Manzi and J. Shuttleworth, 2009b: Evapotranspiration. IGBP Synthesis Vol. *Amazonia and Global Change*. Eds. M. Keller, J. Gash, P. Silva Dias. *Geophys. Monograph Ser.*, **186**.

Freitas, S. R., K.M. Longo, M. Silva Dias, P. Silva Dias, R. Chatfield, E. Prins, P. Artaxo, G. Grell, and F. Recuero, 2005: Monitoring the transport of biomass burning emissions in South America. *Environmental Fluid Mechanics,* **5**(1–2), 135–167, doi: 10.1007/s10652-005-0243-7.

Freitas, S. R., K.M. Longo, and M.O. Andreae, 2006: Impact of including the plume rise of vegetation fires in numerical simulations of associated atmospheric pollutants, *Geophys. Res. Lett.*, **33**, L17808, doi: 10.1029/2006GL026608.

Freitas, S. R., K.M. Longo, R. Chatfield, D. Latham, M.A.F. Silva Dias, M.O. Andreae, E. Prins, J.C. Santos, R. Gielow, and J.A. Carvalho Jr., 2007: Including the sub-grid scale plume rise of vegetation fires in low resolution atmospheric transport models. *Atmos. Chem. Phys.*, **7**, 3385–3398, doi: 10.5194/acp-7-3385-2007.

Freitas, S.R., K.M. Longo, M.A.F. Silva Dias, R. Chatfield, P. Silva Dias, P. Artaxo, M.O. Andreae, G. Grell, L.F. Rodrigues, A. Fazenda and J. Panetta, 2009: The Coupled Aerosol and Tracer Transport model to the Brazilian developments on the Regional Atmospheric Modeling System (CATT-BRAMS) – Part 1: Model description and evaluation. *Atmos. Chem. Phys.*, **9**, 2843–2861, doi: 10.5194/acp-9-2843-2009.

Freud, E., D. Rosenfeld, M.O. Andreae, A. A. Costa, and P. Artaxo, 2008: Robust relations between CCN and the vertical evolution of cloud drop size distribution in deep convective clouds. *Atmos. Chem. Phys.*, **8**, 1661–1675, doi: 10.5194/acp-8-1661-2008.

Fu, R. and W. Li, 2004: The influence of the land surface on the transition from dry to wet season in Amazonia. *Theor. Appl. Clim.*, **78**, 97–110, doi: 10.1007/s00704-004-0046-7.

Fuzzi, S. and 28 co-authors, 2007: Overview of the inorganic and organic composition of size-segregated aerosol in Rondônia, Brazil, from the biomass-burning period to the onset of the wet season. *J. Geophys. Res.*, **112**, D01201, doi: 10.1029/2005JD006741.

Giglio, L., J. Descloitres, C.O. Justice and Y.J. Kaufman, 2003: An enhanced contextual fire detection algorithm for MODIS. *Remote Sensing of Environment,* **87**, 273–282, doi: 10.1016/S0034-4257(03)00184-6.

Gonçalves, F.L.T., J.A. Martins, and M.A. Silva Dias, 2008: Shape parameter analysis using cloud spectra and gamma functions in the numerical modeling RAMS during LBA Project at Amazonian region, Brazil. *Atmos. Res.*, **89**, 1–11, doi: 10.1016/j.atmosres.2007.12.005.

Goulden, M.L., S.D. Miller, H.R. da Rocha, M.C. Menton, H.C. de Freitas, A.M. e Silva Figueira, and C.A.D. de Sousa, 2004: Diel and seasonal patterns of tropical forest CO_2 exchange. *Ecol. Appl.*, **14**(4), supplement, S42–S54, doi: 10.1890/02-6008.

Gu, L., J.D. Fuentes and H.H. Shugart, 1999: Responses of net ecosystem exchanges of carbon dioxide to changes in cloudiness: Results from two North American deciduous forests. *J. Geophys. Res.*, **104**(D24), 31421–31434, doi: 10.1029/1999JD901068.

Gu, L., D. Baldocchi, S.B. Verma, T.A. Black, T. Vesala, E.M. Falge, and P.R. Dowty, 2002: Advantages of diffuse radiation for terrestrial ecosystem productivity. *J. Geophys. Res.*, **107** (D6), 4050, doi: 10.1029/2001JD001242.

Gu, L., D. Baldocchi, S.C. Wofsy, J.W. Munger, J.J. Michalsky, S.P. Urbanski, T.A. Boden, 2003: Response of a Deciduous Forest to the Mount Pinatubo Eruption: Enhanced Photosynthesis. *Science,* **299**, 2035., doi: 10.1126/science.1078366.

Herdies, D.L., A. da Silva, and M.A.F. Silva Dias, 2002: The bi-modal pattern of the summertime circulation over South America. *J. Geophys. Res.*, **107**(D20), doi: 10.1029/2001JD000337.

IPCC, 2007: Intergovernmental Panel on Climate Change – Working Group I: The Physical Science Basis of Climate Change. http://www.ipcc.ch/publications_and_data/ar4/wg1/en/contents.html

Keller, M., A. Alencar, G.P. Asner, B. Braswell, M. Bustamante, E. Davidson, T. Feldpausch, E. Fernandes, M.L. Goulden, P. Kabat, B. Kruijt, F. Luizão, S.D. Miller, D. Markewitz, A.D. Nobre, C.A. Nobre, N. Priante Filho, H.R. da Rocha, P. Silva Dias, C. von Randow, G.L. Vourlitis 2004: Ecological research in the Large scale Biosphere Atmosphere experiment in Amazonia (LBA): early results. *Ecological Applications,* **14**(4): S3–16, doi: 10.1890/03-6003.

Koren, J.V., L.A. Remer, H. Afargan, 2008: Smoke Invigoration Versus Inhibition of Clouds over the Amazon. *Science,* **321**, 5891, 946–949, doi: 10.1126/science.1159185.

LBA, 1996: The Large Scale Biosphere-Atmosphere Experiment in Amazônia (LBA): Concise Experimental Plan. The LBA Science Planning Group. SC–DLO, P.O. Box 125, 6700 AC Wageningen, The Netherlands, 44 pp.

Lin, J. C., T. Matsui, R.A. Pielke, Sr. and C. Kummerow, 2006: Effects of biomass burning-derived aerosols on precipitation and clouds in the Amazon Basin: A satellite-based empirical study. *J. Geophys. Res.,* **111**, (D19204), doi: 10.1029/2005JD006884.

Longo, K.M., S.R. Freitas, A. Setzer, E. Prins, P. Artaxo, and M.O. Andreae, 2007: The Coupled Aerosol and Tracer Transport model to the Brazilian developments on the Regional Atmospheric Modeling System (CATT-BRAMS) – Part 2: Model sensitivity to the biomass burning inventories. *Atmos. Chem. Phys. Discuss.,* **7**, 8571–8595, doi: 10.5194/acpd-7-8571-2007.

Longo, K.M., S.R. Freitas, M.O. Andreae, R. Yokelson and P. Artaxo, 2009: Biomass burning in Amazonia: emissions, long-range transport of smoke and its regional and remote impacts. IGBP Synthesis Vol. *Amazonia and Global Change*. Eds. M. Keller, J. Gash, P. Silva Dias. *Geophys. Monograph Ser.,* **186**.

Mahli, Y., D.D. Baldochi, P.G. Jarvis, 1999: The carbon balance of tropical, temperate and boreal forests. *Plant, Cell and Environment,* **22**, 715–740, doi: 10.1046/j.1365-3040.1999.00453.x.

Marengo, J., C.A. Nobre, R.A. Betts, P.M. Cox, G. Sampaio and L. Salazar, 2009: Global Warming and Climate Change in Amazonia: Climate-Vegetation Feedback and Impacts on Water Resources. IGBP Synthesis Vol. *Amazonia and Global Change*. Eds. M. Keller, J. Gash, P. Silva Dias. *Geophys. Monograph Ser.,* **186**.

Martins, J.A., and M.A.F. Silva Dias, 2009: The impact of smoke from forest fires on the spectral dispersion of cloud droplet size distributions in the Amazonian region. *Environmental Res. Lett.,* **4**, doi: 10.1088/1748-9326/4/1/015002.

Martins, J.A., M.A.F. Silva Dias, and F.L.T. Gonçalves, 2009a: Impact of biomass burning aerosols on precipitation in the Amazon: A modeling case study. *J. Geophys. Res.,* **114**, D02207, doi: 10.1029/2007JD009587.

Martins, J.A., F.L.T. Gonçalves, C.A. Morales, G.F. Fisch, F.G. M. Pinheiro, J.B.V. Leal Júnior, C.J. Oliveira, E.M. Silva, J.C.P. Oliveira, A.A. Costa and M.A.F. Silva Dias, 2009b: Cloud condensation nuclei from biomass burning during the Amazonian dry-to-wet transition season. *Meteorol. Atmos. Physics,* **104**, 83–93, doi: 10.1007/s00703-009-0019-6.

Miller, S. D., M.L. Goulden, M.C. Menton, H.R. da Rocha, H.C. de Freitas, A.M.E.S. Figueira, and C. A.D. de Sousa, 2004: Biometric and micrometeorological measurements of tropical forest carbon balance. *Ecol. Appl.,* **14**(4), supplement, S114–S126, doi: 10.1890/02-6005.

Morcrette, J.-J., O. Boucher, L. Jones, D. Salmond, P. Bechtold, A. Beljaars, A. Benedetti, A. Bonet, J.W. Kaiser, M. Razinger, M. Schulz, S. Serrar, A.J. Simmons, M. Sofiev, M. Suttie, A.M. Tompkins, A. Untch, 2009: Aerosol analysis and forecast in the ECMWF Integrated Forecast System: Forward modeling. *J. Geophys. Res.,* **114**, D06206, doi: 10.1029/2008JD011235.

Nepstad, D.C., C.R. de Carvalho, E.A. Davidson, P.H. Jipp, P.A. Lefebvre, G.H. Negreiros, E.D. da Silva, T.A. Stone, S.E. Trumbore, and S.Vieira, 1994: The role of deep roots in the hydrological and carbon cycles of Amazonian forest and pastures. *Nature,* **372**, 666–669, doi: 10.1038/372666a0.

Niyogi, D., *et al.,* 2004: Direct observations of the effects of aerosol loading on net ecosystem CO_2 exchanges over different landscapes, *Geophys. Res. Lett.,* **31**, L20506, doi: 10.1029/2004GL020915.

Nobre, C.A., G.O. Obregón and J. A. Marengo, 2009: Characteristics of Amazonian climate: main features. IGBP Synthesis Vol. *Amazonia and Global Change*. Eds. M. Keller, J. Gash, P. Silva Dias. *Geophys. Monograph Ser.,* **186**.

Oliveira, R.S., T.E. Dawson, S.S.O. Burgess, and D.C. Nepstad, 2005: Hydraulic redistribution in three Amazonian trees. *Oecologia,* **145**, 354–363, doi: 10.1007/s00442-005-0108-2.

Oliveira, P.H.F., P. Artaxo, C. Pires, S. De Lucca, A. Procopio, B. Holben, J. Schafer, L.F. Cardoso, S.C. Wofsy and H.R. Rocha, 2007: The effects of biomass burning aerosols and clouds on the CO_2 flux in Amazonia. *Tellus B*, **59**, 338–349, doi: 10.1111/j.1600-0889.2007.00270.x.

Prins, E., J. Feltz, W. Menzel, and D. Ward, 1998: An overview of GOES-8 diurnal fire and smoke results for SCAR-B and 1995 fire season in South America. *J. Geophys. Res.,* **103**(D24), 31,821–31,835, doi: 10.1029/98JD01720.

Rickenbach, T.M., R. Nieto Ferreira, J. Halverson, D.L. Herdies, and M.A.F. Silva Dias, 2002: Modulation of convection in the southwestern Amazon basin by extratropical stationary fronts. *J. Geophys. Res.,* **107**, 8040, doi: 10.1029/2000JD000263.

Roberts, J., O.M.R. Cabral, G. Fisch, L. C.B. Molion, C.J. Moore, W.J. Shuttleworth, 1993: Transpiration from an Amazonian rainforest calculated from stomatal conductance measurements. *Agric. Forest Meteorol.,* **65**, 175–196, doi: 10.1016/0168-1923(93)90003-Z.

Saleska, S.R. and 17 co-authors, 2003: Carbon in Amazon Forests: Unexpected Seasonal Fluxes and Disturbance-Induced Losses. *Science,* **302**, 1554–1557, doi: 10.1126/science.1091165.

Saleska, S. R., K. Didan, A. R. Huete, and H. R. da Rocha, 2007: Amazon forests green-up during 2005 drought. *Science,* **318**, 612, doi: 10.1126/science.1146663.

Setzer, A. and M. Pereira, 1991: Amazonia biomass burnings in 1987 and an estimate of their tropospheric emissions. *Ambio.,* **20**, 19–22.

Silva Dias, M.A.F., R. Avissar, P.L. Silva Dias, 2009: Modeling the Regional and Remote Climatic Impact of Deforestation. IGBP Synthesis Vol. *Amazonia and*

Global Change. Eds. M. Keller, J. Gash, P. Silva Dias. *Geophys. Monograph Ser.*, **186**.

Uppala, S. M., *et al.*, 2005: The ERA-40 re-analysis. *Q. J. R. Meteorol. Soc.*, **131**, 2961–3012, doi: 10.1256/qj.04.176.

Uppala, S., D. Dee, S. Kobayashi, P. Berrisford, and A. Simmons, 2008: Towards a climate data assimilation system: Status update of ERA-Interim. *ECMWF Newsletter*, **115**, pp. 12–18, European Centre for Medium-Range Weather Forecasts, Reading, UK. (Available at http://www.ecmwf.int/publications/newsletters)

Vendrasco, E.P., P.L. Silva Dias, E.D. Freitas, 2009: A case study of the direct radiative effect of biomass burning aerosols on precipitation in the Eastern Amazon. *Atmos. Res.*, **94**, 409–421, doi: 10.1016/j.atmosres.2009.06.016.

von Randow, C.A., O. Manzi, B. Kruijt, P.J. de Oliveira, F.B. Zanchi, R.L. Silva, M.G. Hodnett, J.K.C. Cash, J.A. Elbers, M.J. Waterloo, F.L. Cardoso and P. Kabat, 2004: Comparative measurements and seasonal variations in energy and carbon exchange over forest and pasture in south west Amazonia. *Theor. Appl. Climatol.*, **78**, 5–26, doi: 10.1007/s00704-004-0041-z.

Wang, J., F.J.F. Chagnon, E. Williams, A.K. Betts, N.O. Renno, L.A.T. Machado, G. Bisht, R. Knox and R.L. Bras, 2009: Impact of deforestation in the Amazon basin on cloud climatology. *PNAS*, doi: 10.1073/pnas.0810156106.

Williams, E. and 32 co-authors, 2002: Contrasting convective regimes over the Amazon: Implications for Cloud Electrification. *J. Geophys. Res.*, **107**, 8082, doi: 10.1029/2001JD000380.

Zhang, Y., R. Fu, H. Yu, Y. Qian, R. Dickinson, M.A.F. Silva Dias, P.L. da Silva Dias, and K. Fernandes, 2009: Impact of biomass burning aerosol on the monsoon circulation transition over Amazonia. *Geophys. Res. Lett.*, **36**, L10814, doi: 10.1029/2009GL037180.

Zhang, Y.-C., W.B. Rossow, A.A. Lacis, V. Oinas, and M.I. Mishchenko, 2004: Calculation of radiative fluxes from the surface to top of atmosphere based on ISCCP and other global data sets: Refinements of the radiative transfer model and the input data. *J. Geophys. Res.*, **109**, D19105, doi: 10.1029/2003JD004457.